In situ electronic structural study of VO_2 thin film across the metal–insulator transition*

Emin Muhemmed(伊明江 · 买买提), Abduleziz Ablat(阿布都艾则孜 · 阿布来提), Wu Rui(吴 蕊), Wang Jia-Ou(王嘉鸥), Qian Hai-Jie(钱海杰), and Kurash Ibrahim(奎热西 · 依布拉欣)†

Institute of High Energy Physics, Chinese Academy of Sciences, Beijing 100049, *China*

(Received 7 March 2013; revised manuscript received 14 April 2013)

The *in situ* valence band photoemission spectrum (PES) and X-ray absorption spectrum (XAS) at V $L_{II} - L_{III}$ edges of the VO_2 thin film, which is prepared by pulsed laser deposition, are measured across the metal–insulator transition (MIT) temperature ($T_{MIT} = 67$ °C). The spectra show evidence for changes in the electronic structure depending on temperature. Across the T_{MIT}, pure V 3d characteristic $d_{\|}$ and O 2p-V 3d hybridization characteristic π_{pd}, σ_{pd} bands vary in binding energy position and density of state distributions. The XAS reveals a temperature-dependent reversible energy shift at the V L_{III}-edge. The PES and XAS results imply a synergetic energy position shift of occupied valence bands and unoccupied conduction band states across the phase transition. A joint inspection of the PES and XAS results shows that the MIT is not a one-step process, instead it is a process in which a semiconductor phase appears as an intermediate state. The final metallic phase from insulating state is reached through insulator–semiconductor, semiconductor–metal processes, and *vice versa*. The conventional MIT at around the $T_{MIT} = 67$ °C is actually a semiconductor–insulator transformation point.

Keywords: vanadium dioxide, metal–insulator transition, electronic structure, photoemission spectroscopy

PACS: 71.30.+h, 79.60.–I, 78.70.Dm, 73.20.At **DOI:** 10.1088/1674-1056/22/12/127103

1. Introduction

Vanadium dioxide exhibits a remarkable characteristic that undergoes a metal–insulator transition (MIT) at close to room temperature at $T_{MIT} = 67$ °C.[1] Accompanied by MIT, the system goes through a lattice transformation[2] from a tetragonal structure of the metallic phase above the T_{MIT} to a monoclinic structure of the insulating phase below the T_{MIT}. These properties have been under exploration for advanced electric device technological applications,[3,4] as well as being a hotbed of finding new aspects across the MIT.[5] Remarkable changes in the electrical and optical properties with the MIT,[5,6] make it an attractive material for application in switches, sensors, and smart optical windows.[7–10] MIT in the system has been studied for decades and is still not fully understood. This can partly be attributed to the fact that the microscopic relation between the electronic structure and the crystal structure across the MIT still remains an issue not yet concluded.

Concerning the origin of the MIT phenomenon in VO_2, there is a model which suggests that the system experiences unit-cell distortion and a strong electron–lattice coupling driven Peierls-type transition.[11] Where under the octahedral crystal field, the degeneracies of the highest occupied three t_{2g} orbitals are completely removed and split into two d_{π}, which hybridize with the O 2p to form π_{pd} and π^*_{pd} bands, and an occupied $d_{\|}$ orbital left free (non-bonding) and parallel to the lattice *c* direction. In the insulating phase of monoclinic crystal structures at low-*T*, the formation of zigzag-type V–V dimers lifts the π^*_{pd} band to above the Fermi level (E_F); the occupied $d_{\|}$ band splits into a lower filled free non-bonding $d_{\|}$ band and an upper empty antibonding $d^*_{\|}$ band, then a gap appears between the filled free $d_{\|}$ and π^*_{pd} bands. In the metallic phase above T_{MIT}, the V–V dimers evolve into chainlike $[V–V]_n$ clusters, the occupied and unoccupied $d_{\|}$ bands merge, they then evolve into $d^*_{\|} + d^1_{\|}$ bands and the $d^1_{\|}$ overlap with the π^*_{pd} band, so the band gap closes.

It is important to understand the microscopic relation between the electronic and crystal structures of the observed MIT phenomenon in terms of the electronic structure. Accounting for the importance of electron–electron correlations in VO_2, the MIT is attributed to an on-site Hubbard-type Coulomb energy in the $d_{\|}$ bands.[12] The gap value is also obtained in the cluster dynamical mean-field theory,[13] showing the importance of both the Coulomb interaction and structural distortions in VO_2. In this work, the VO_2 thin film is systematically studied by the valence band photoemission spectrum (PES) and V $L_{II,III}$ edge X-ray absorption spectrum (XAS). The investigation is to inspect the electronic structural evolution with a cyclic variation of temperature to look particularly at how the electronic structural parameters, such as binding energy positions, density of states of bands, and interatomic correlations, are regulated across the phase transition. At the end of the discussion, we show that the microscopic electronic structural change perfectly matches with the elegant results in the macroscopic electrical resistance and resistivity measurement on the

*Project supported by the Natural Science Foundation of the Chinese Academy of Sciences (Grant No. H91G750Y21).

†Corresponding author. E-mail: kurash@ihep.ac.cn

© 2013 Chinese Physical Society and IOP Publishing Ltd

size of the well-defined nanobeams, observed as a function of T.

2. Experiment

The VO_2 thin film was grown on a Si substrate by means of pulsed-laser deposition through ablating the target at an ambient oxygen pressure 8×10^{-3} Pa, keeping the substrate at 550 °C during the deposition. The thin film growth, the valence PES, and XAS measurements were performed *in situ* at the beam line 4B9B of the Beijing Synchrotron Radiation Facility. The PESs are fitted with XPSPeak4.1.[14] A Shirley background and a mixed Lorentzian–Gaussian line shape were employed for the peak-fit. The temperature measurement during PES and XAS data acquisition was completed through a thermocouple welded on a manipulator very close to the sample holder; the manipulator contacts very well with the sample holder so the temperature read-off then was taken to be equal to the actual temperature of the sample.

3. Results and discussion

Valence band spectra reveal the information about the density of states of electrons in valence band, which in vanadium dioxide consist of V 4s, V 3d, and O 2p orbital electrons. The resulting bands $d_{\|}$, $d^{*}_{\|} + d^{1}_{\|}$, π_{pd}, σ_{pd} and σ_{sp} near the Fermi level are given in Fig. 1 where schematically shown are the band structures for both the insulating and metallic phases following their classification by Goodenough.[11] The peak designation from near the Fermi level to below follows the molecular orbital model and experimental report.[15,16] The free V 3d characteristic states $d^{1}_{\|}$ and $d^{*}_{\|}$ in the metallic phase were termed coherent and incoherent bands respectively.[17] The coherent band $d^{1}_{\|}$ is one of the electron characteristics, overlapping with the $d^{1}_{\|}$ C conduction band state near Fermi edge and the incoherent band $d^{*}_{\|}$, with the property of plasmon-like excited band states $d^{n+1}_{\|} + d^{n-1}_{\|}$ formed by an interatomic exchange interaction between degenerate $d^{n}_{\|}$ bands as a result of the increased degeneracy of the vanadium ions with heating in the clustered $[V–V]_n$ chains.[17] The π_{pd} is for bonding plus nonbonding π-type electron bands of V 3d–O 2p hybridization, the σ_{pd} is for V 3d–O 2p hybridization, and the σ_{sp} for V 4s–O 2p hybridization σ-type bands.

Figure 2(a) shows the VO_2 valence band PESs measured at 25 °C and 140 °C, the former is in an insulating state and the latter is in a metallic state. A comparison of the two spectra shows an energy gap of about 0.2 eV, which is defined as the energy difference between the Fermi level of the metallic state and the top edge of the valence band of the insulating state in the same system.[18] The observed energy gap is comparable to those measured by PES[18] and hard X-ray XPS.[15] Figure 2(b) shows the peak fitting results from Fig. 2(a), where the $d_{\|}$ peak at low-T evolves into the $d^{*}_{\|} + d^{1}_{\|}$ two-peak feature at high-T with binding energies at 1.26 eV and 0.6 eV, correspondingly. The numerical results of the spectra fitting are listed in Table 1, where the values of E_B are the binding energy values of the peaks $d_{\|}$, $d^{1}_{\|}$, $d^{*}_{\|}$, ($d^{*}_{\|} + d^{1}_{\|}$ as a whole), π_{pd}, σ_{pd}, and σ_{sp} at the temperatures below and above the T_{MIT}, the FWHM is the full width at half maximum, and the $i/\sum i$ is the i-th peak's relative intensity.

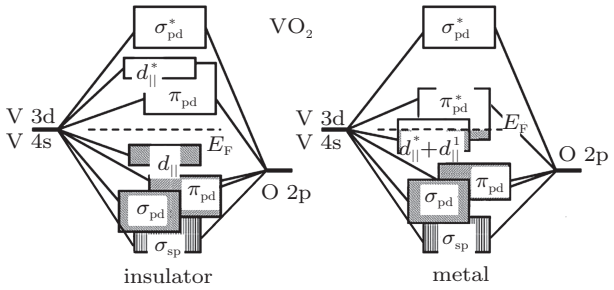


Fig. 1. Schematic orbital hybridization and split of VO_2 bands near the Fermi level in metallic and insulating phases following the report in Ref. [11].

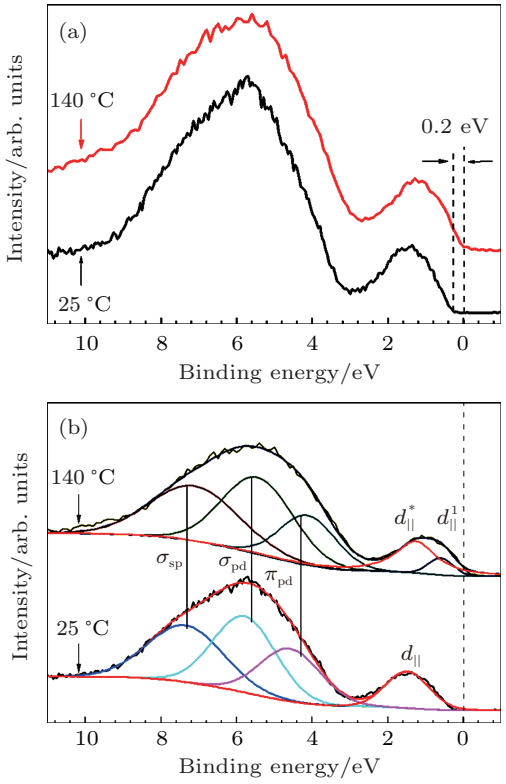


Fig. 2. (color online) (a) Valence-band spectra measured across the MIT at $h\nu = 40$ eV and the band gap. (b) Fitting results of the spectra in panel (a).

Figures 2(a) and 2(b) and the values in Table 1 show that the peaks' binding energies, intensities and the FWHMs change along with the phase transition. The difference in these three parameters for the same peak in different phase spaces shows the background story of the phase transition. The change in the peak energy position provides important relationship information between the electronic structure and the crystal structure along with the temperature

variation. It is also an indicator for the variation in the potential energy of the electrons in a band state, the decrease in E_B implies an increase in potential energy. The binding (or potential) energy values of all the peaks $d_{\|}^{l}$, $d_{\|}^{*}$, $d_{\|}^{*}+d_{\|}^{l}$,

Table 1. Fitting results extracted from Fig. 2(b). The peak is represented by i; T (°C) is the temperatures at which the spectra were measured; E_B (eV) is the corresponding peak's binding energy; FWHM is the full width at half maximum of the corresponding peak; $i/\sum i$ is the relative intensity ratio of the i-th peak $d_{\|}$, $d_{\|}^{*}$, $d_{\|}^{l}$, $d_{\|}^{*}+d_{\|}^{l}$, π_{pd}, σ_{pd}, and σ_{sp} to their sum $\sum i$ at respective temperatures.

i	$d_{\|}$	$d_{\|}^{*}$	$d_{\|}^{l}$	$d_{\|}^{*}+d_{\|}^{l}$	π_{pd}		σ_{pd}		σ_{sp}	
T/°C	25	140	140	140	25	140	25	140	25	140
E_B/eV	1.28	1.26	0.6	1.03	4.38	4.12	5.59	5.45	7.16	7.12
FWHM	1.36	1.28	0.78	1.50	1.9	1.74	1.95	2.21	2.35	2.75
$i/\sum i$	0.11	0.12	0.03	0.15	0.23	0.17	0.34	0.36	0.32	0.32

π_{pd}, and σ_{pd}, except that of σ_{sp}, decrease (or upshift) and shift toward Fermi edge ~0.2 eV when the system transforms from an insulating phase to a metallic state, this is in accordance with the calculated crystal structural distortion-induced energy upshift of ~0.162 eV from monoclinic to tetragonal.[19] In terms of the potential energy variation, the unidirectional upshifts of all of the band positions imply a generic situation where the system transforms from a rather stable state at low-T to a less stable one at high-T.

Concerning the relations between band states, the relative intensity $i/\sum i$ and the FWHM are two closely interrelated parametres that reflect in-band electron numbers and the extent of their spatial distribution, respectively. These two parameters directly relate to the variation in the chemical bonding environment and the bonding characteristics of the bands between atoms. Keeping intact of σ_{sp} implies that the electrons in this deeper lying band state are almost not related to the phase transition. The parameters of the rest $d_{\|}^{l}$, $d_{\|}^{*}$, $d_{\|}^{*}+d_{\|}^{l}$, π_{pd}, σ_{pd} bands show that they are the active players and major contributors to the MIT process. Accross the phase transition, both the $i/\sum i$ and FWHM of the $d_{\|}^{l}$, $d_{\|}^{*}$, $d_{\|}^{*}+d_{\|}^{l}$, π_{pd}, and σ_{pd} bands experience variations.

By definition,[17] the different ratio of U_{dd} to W characterizes either the insulating or metallic phase of a system, i.e., the system is metallic when $U_{dd}/W < 1$ and becomes insulating when $U_{dd}/W > 1$, where U_{dd} is the on-site d–d Coulomb repulsion between the V–V ions and W is the d electron band width. If one would relate the U_{dd} and W to an experimental observation, one could take the E_B analogous to U_{dd} and FWFM to W, where $E_B \propto U_{dd}$ and FWHM $\propto W$. Across the T_{MIT}, the observed most prominent change occurs for the single occupied $d_{\|}$ band that splits into occupied coherent $d_{\|}^{l}$ and incoherent $d_{\|}^{*}$ bands at the high-T phase. From the values in Table 1, both the E_B (1.28 eV) and FWHM (1.36 eV) of the $d_{\|}$ band at low-T change to the weighed 1.03 eV and 1.50 eV of $d_{\|}^{*}+d_{\|}^{l}$ band at high-T; at the same time, the change is accompanied by a slight increase in the total electron density of states in the $d_{\|}^{*}+d_{\|}^{l}$ band. The estimated $U_{dd}/W \propto 1.28/1.36 = 0.94$ for the insulating phase and $U_{dd}/W \propto 1.03/1.50 = 0.69$ for the metallic state imply an apparent agreement of the observation with the theoretical requirement for the two phases. The metallic state then can be described as being due to the decrease of the U_{dd} between V–V ions with the increase of d–d degeneracy by the formation of $[V–V]_n$ chainlike clusters. These variations result in the transition of the free electron like $d_{\|}$ band from a localized state at low-T in the V–V dimers to delocalized split states at high-T in the $[V–V]_n$ clusters.

The observed π_{pd} and σ_{pd} band results imply that they are also extremely sensitive to the symmetry changes of the crystal structure; their binding energies upshift toward the Fermi edge with a larger magnitude than others when the system transforms from monoclinic to tetragonal symmetry. While the intensity and peak width of the π_{pd} band decrease from low-T through high-T phase, whereas the intensity and peak width of the σ_{pd} band increase. These variations reveal a complicated but still clear situation, which is in contrast to that of the $d_{\|}$ band. The observed changes of the parameters imply that there is an electron density renormalization mechanism among the $d_{\|}$, $d_{\|}^{*}+d_{\|}^{l}$, π_{pd}, and σ_{pd} bands through MIT, as will be discussed below.

If one takes a position in the center π_{pd} band as the leverage supporting point between the upper side $d_{\|}^{*}+d_{\|}^{l}$ and lower side σ_{pd} bands, one can find that the variation of π_{pd}'s three parameters along with the phase transition lead to a coordinated density of state redistributions between the two $d_{\|}^{*}+d_{\|}^{l}$ and σ_{pd} bands and a slight modification of the corresponding bond characteristics. Despite the fact that all three $d_{\|}^{*}+d_{\|}^{l}$, π_{pd}, σ_{pd} bands translate to higher potential energy positions at high-T, the π_{pd} band's density of states decreases and its FWHM narrows at high-T, the same parameters of the $d_{\|}^{*}+d_{\|}^{l}$, σ_{pd} bands at the two sides gain apparently increased weights. This fact can be described as the two neighboring side $d_{\|}^{*}+d_{\|}^{l}$, σ_{pd} bands that strip some portion of the density of states of the π_{pd} band at high-T and *vice versa* for the π_{pd} band from two neighboring sides at low-T. In this process, the increase in the density of states in the σ_{pd} band and in the free nonbonding

$d_{\|}^{*} + d_{\|}^{1}$ bands is compensated by the decrease of the same parameters of the π_{pd} band at high-T and *vice versa* at low-T in a reversible way.

Figure 3 shows XAS results at V L_{II}–L_{III} edges across the T_{MIT} with thermal heating of the sample from 25 °C to 140 °C and then cooling down to 35 °C. The reason why the PESs did not show experimentally a performance similar to XASs over a varied temperature is given in the last section. The V L_{II}–L_{III} XASs result in the electron transitions of 2p to 3d unoccupied states[20] following the dipole electric selection requirements $\Delta l = \pm 1$. The two pronounced maxima at 517 eV and 523.6 eV correspond to the spin–orbit split levels $2p_{3/2}$ and $2p_{1/2}$, respectively. The presence or absence of the shoulder at ~515 eV has been taken to be a touchstone to judge whether the sample is in a single crystal structure or in a polycrystalline form.[21] The results confirm that the thin film is in the single crystalline form.

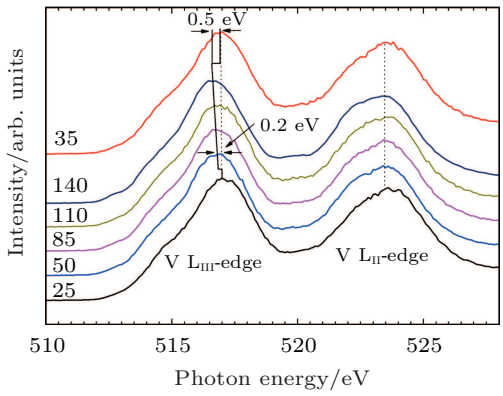


Fig. 3. (color online) Temperature-dependent evolutions of XAS at V L_{II}–L_{III} edges, the temperature increases from initial 25 °C to the highest point 140 °C by heating and then ends at 35 °C by cooling down.

Along with the warming, the V $2p_{3/2}$ maximum position at 517 eV jumps at first rather drastically to a lower photon energy position at the nominal 50 °C than that at room temperature and downshifts further continuously toward lower photon energies with a total energy shift of ~0.5 eV at 140 °C, then returns to the 517 eV position when the sample cools down to 35 °C. While the $2p_{3/2}$ edge position experiences back and forth oscillation across the T_{MIT} against thermal cycling, the $2p_{1/2}$ energy position stays almost unchanged. The XAS position change at both the O 1s and V 2p edges across the T_{MIT} was observed before,[20,22] but the question that has not yet been touched on is what information might be revealed if one inspects jointly the PES and XAS.

The observed conduction band lowering in XAS with the thermal heating implies that it is a static follow-up process mediated by adjusting the density of state distributions as a response to the crystal structural deformation. Combining the PES and XAS results together, one can have a deeper insight into the observed reversible mechanism of the metallic Fermi state and the insulating band-gap formation. Together with the valence band shift of 0.2 eV observed at the leading edges of the PES shown in Fig. 2, which keeps intact with temperature[15,18,22] but at the same time a sequential band gap variation is observed in the XASs in Fig. 3 from about 0.2 eV lowering in the conduction band state at the phase transition T_{MIT} to the highest 0.5 eV lowering at above 110 °C, we thus deduce an intermediate optical band gap that is 0.2 eV + 0.2 eV ≈ 0.4 eV at the T_{MIT} and a largest optical band gap that is 0.2 eV + 0.5 eV ≈ 0.7 eV for the system at the low-T phase. The last value is in good agreement with the measurement results of the optical band gap and the semiconducting band gap.[19,21] This largest optical band gap value 0.7 eV implies that if the insulator VO_2 were metal, it would have closed the 0.7 eV band gap, otherwise due to the difference 0.7 eV − 0.4 eV = 0.3 eV from T_{MIT} to above 110 °C, the system would not be a metal at the conventional T_{MIT} point.

In the underlying system, the PES and XAS results manifest that both occupied and unoccupied band states respectively offer information about both the highest occupied valence band state and the lowest unoccupied conduction band state, moving in the manner of head-to-head in the opposite directions to close up the band gap when heated. Apparently, the two bands lean apart when cooled down to open the band gap. The continuous variation of the gap between the conduction band observed in the XAS and the intact valence band edge in the PES poses a further question on the origin of the phase transition and implies that the MIT actually is not reached from the insulator to the metal phase at one step just at the T_{MIT}, instead the phase transition process is continuing with the temperature from T_{MIT} until the system turns into a metallic state above 110 °C. These all point to the MIT going through a semiconductor state as being an intermediate transit phase between the metal and insulator phases, as will be discussed below.

The above PES and XAS results, especially the XAS results, clearly show that the phase state evolution of the VO_2 does not stop at the fixed T_{MIT} point during the temperature increasing (or decreasing) as the valence band edge does in the PES after the system has passed through the T_{MIT}. Leading edge positions for both metal and semiconductor phases, the Fermi band edge and valence band edge respectively in the two systems usually do not change with the temperature in the PES measurement as soon as they emerge from their predecessor insulator phase by closing a band gap. Like the usual PES results in the reports,[15,18,22] this PES for the valence band

edge energy position remains intact with the temperature increasing until 140 °C after closing up the 0.2 eV band gap at the T_{MIT}. The XAS results are usually taken to be a direct reflection of the conduction band status, due to their interpretation of the electron excitation–de-excitation processes as being an initially excited core electron first jumping into an unoccupied conduction band, then the excited state is de-excited into final states through Auger-like, photoemission-like or autoionization processes. What is interesting in our XAS results is that the energy position varies continuously after the T_{MIT}. This variation is most closely related to the conduction band state of the system, implying that there exists a gap between the highest occupied valence band edge and the lowest unoccupied conduction band edge. This kind of variation is not expected for the metallic phase because when the two edges overlap in the metallic state to form the Fermi edge, the XAS should stay intact during the temperature variation. In the XAS in Fig. 3, the gap between the valence band edge and the lowest conduction band edge changes 0.5 eV − 0.2 eV = 0.3 eV from T_{MIT} to 140 °C. In other words, when the system occurs, the said MIT takes place at T_{MIT}, it still has a distance 0.7 eV − 0.4 eV = 0.3 eV to reach its metallic phase. Then the 0.3 eV difference has to be eliminated by further increasing the temperature. Here, the number 0.4 eV is the sum of closed gap values 2×0.2 eV measured from both the valence band edge in the PES and in the XAS at T_{MIT}, as indicated in Figs. 2 and 3, respectively. What is further needed is to eliminate the 0.3 eV gap after the MIT by increasing the temperature, which implies that the system experiences a process with characteristics pertaining neither to an insulator nor to a metallic phase; it can only be attributed to a semiconductor phase state for the path from the T_{MIT} to the final metallic phase at ∼140 °C. The XAS observation fits only to a semiconductor band gap interpretation due to the fact that the metallicity increases with heating. This conclusion from the XAS result provides a natural support to an earlier electric resistivity and resistance measurement carried out on VO_2 nanobeams,[5] as will be discussed below.

The temperature dependence of the electrical resistivity, which is a macroscopic property of material, offers clues to the behavior of microscopic electrical carriers. The electric resistance measurement of a micrometer length of VO_2 nanobeams with temperature variation demonstrates a similar tendency[5] to our observed electronic structure evolution. The XAS behavior at the V $2p_{3/2}$ edge, i.e., its drastic jump down in the excitation photon energy first at ∼50 °C and a continuous decrease of the peak position with the temperature increase, is similar to the observation of electrical resistance variation across the T_{MIT} of vanadium dioxide nanobeams. The observed results shown as the insulating fraction variation x versus the temperature for suspended nanobeams of various dimensions and the resistance variation versus the temperature, show that both the insulating fraction and the electrical resistance decrease drastically at or below 68 °C during heating and then they decrease linearly and continuously with the temperature increasing, i.e., the metallicity is enhanced continuously with heating. These perfect matches of the microscopic electronic state variation with the macroscopic property change further confirm that those observations from the XAS are the generic behavior of the semiconductor-to-metallic phase.

4. Conclusion

In this paper, the PES results show a close relationship among $d_{\|}$, π_{pd}, and σ_{pd} bands across the MIT. The temperature dependence merges and splits the circulation between the $d_{\|}$ and $d^{*}_{\|} + d^{1}_{\|}$ bands across the T_{MIT}, demonstrating an alternative localization and delocalization of d band electrons between the insulating and metallic phases. The enhanced σ_{pd} bond at high-T phase has been reached at the expense of weakening the π_{pd} bond and *vice versa* for the π_{pd} state at the low-T phase. The temperature-dependent properties of the XAS across the T_{MIT} reveal reversible energy shifts at the V L_{III}-edge. The joint inspection of PES and XAS implies that the metallic Fermi state formation and the insulating band gap appearance actually result in the synergetic head-to-head closing and tail-to-tail shift apart of the occupied and the lowest unoccupied states, respectively. The deduced band gap from XAS–PES spectra well reproduces the reported optical and semiconducting band gaps. The observed microscopic quantum-level electronic structural variation matches perfectly with the literature-reported macroscopic electric resistivity change as a function of T. All these results pinpoint the fact that the conventional MIT at around $T_{MIT} = 67$ °C is actually a semiconductor–insulator phase transition, the metal–insulator transition occurs when the temperature is further increased to above 110 °C.

References

[1] Morin F G 1959 *Phys. Rev. Lett.* **3** 34

[2] Imada M, Fujimori A and Tokura Y 1998 *Rev. Mod. Phys.* **70** 1039

[3] Driscoll T, Palit S, Qazilbash M M, Brehm M, Keilmann F, Chae B G, Yun S J, Kim H T, Cho S Y, Jokerst N M, Smith D R, and Basov D N 2008 *Appl. Phys. Lett.* **93** 024101

[4] Chen C H and Zhou Z P 2007 *Appl. Phys. Lett.* **91** 011107

[5] Wei J, Wang Z H, Chen W and Cobden D H 2009 *Nat. Nanotechnol.* **4** 420

[6] Wang T, Jiang Y D, Yu H, Wu Z M and Zhao H N 2011 *Chin. Phys. B* **20** 038101

[7] Wang Z M, Ma Y L, Zhang F J and Feng Y D 2007 *Chin. Phys.* **16** 1704
[8] Wang H C, Yi X J, Lai J J and Li Y 2005 *Chin. Phys. Lett.* **22** 1746
[9] Manning T D, Parkin I P, Pemble M E, Sheel D and Vernardou D 2004 *Chem. Mater.* **16** 744
[10] Wei X Y, Hu M, Zhang K L, Wang F, Zhao J S and Miao Y P 2013 *Chin. Phys. B* **22** 037201
[11] Goodenough J B 1971 *J. Solid State Chem.* **3** 490
[12] Zylbersztejn A and Mott N F 1975 *Phys. Rev. B* **11** 4383
[13] Biermann S, Poteryaev A, Lichtenstein A I and Georges A 2005 *Phys. Rev. Lett.* **94** 026404
[14] Kwork R, XPS peak version 4.1, a software was used to analyze the XPS spectra, http://www.phy.cuhk.edu.hk/surface/XPSPEAK/
[15] Eguchi R, Taguchi M, Matsunami M, Horiba K, Yamamoto K, Ishida Y, Chainani A, Takata Y, Yabashi M, Miwa D, Nishino Y, Tamasaku K, Ishikawa K, Senba Y, Ohashi H, Muraoka Y, Hiroi Z and Shin S 2008 *Phys. Rev. B* **78** 075115
[16] Kurmaev E Z, Cherkashenko V M, Yarmoshenko Y M, Bartkowski S, Postnikov A V, Neumann N, Duda L C, Guo J H, Nordgren J, Perelyaev V A and Reichelt W 1998 *J. Phys.: Condens. Matter* **10** 4081
[17] Fujimori A, Hase I, Namatame H, Fujishima Y, Tokura Y, Eisaki H, Uchida S, Takegahara K and de Groot F M F 1992 *Phys. Rev. Lett.* **69** 1796
[18] Shin S, Suga S, Taniguchi M, Fujisawa M, Kanzaki H, Fujimori A, Daimon H, Ueda Y, Kosuge K and Kachi S 1990 *Phys. Rev. B* **41** 4993
[19] Liu L, Cao F, Yao T, Xu Y, Zhou M, Qu B Y, Pan B C, Wu C Z, Wei S Q and Xie Y 2012 *New J. Chem.* **36** 619
[20] Cavalleri A, Rini M, Chong H H W, Fourmaux S, Glover T E, Heimann P A, Kieffer J C and Schoenlein R W 2005 *Phys. Rev. Lett.* **95** 067405
[21] Ruzmetov D, Senanayake S D and Ramanathan S 2007 *Phys. Rev. B* **75** 195102
[22] Koethe T C, Hu Z, Haverkort M W, Schüßler-Langeheine C, Venturini F, Brookes N B, Tjernberg O, Reichelt W, Hsieh H H, Lin H J, Chen C T and Tjeng L H 2006 *Phys. Rev. Lett.* **97** 116402